Elastic-Surface-Wave Scattering from Point-Mass Defects in a Solid Surface

Tetsuro Sakuma
Department of Engineering Science, Hokkaido University, Sapporo, Japan
(Received 27 November 1972)

Scattering of elastic surface waves from static mass defects in a solid surface is investigated by means of field-theoretical scattering theory. All modes of elastic surface waves constructing an orthonormal complete set are involved to calculate the scattering cross sections as functions of frequency for incident Rayleigh-mode waves. It is shown that those cross sections except $\sigma_{R\text{-}SH}$ reveal the characteristic resonance structure in the frequency region $\omega \simeq (0.5\text{–}4.0)\times 10^{13}$ sec^{-1}. The author also finds that the rescattering effects significantly enhance the scattering into other Rayleigh-mode waves.

I. INTRODUCTION

Recently, the quantum of elastic surface waves has become the subject of considerable interest in understanding the transport properties of electrons in the semiconductor inversion layer.[1] Quantization of elastic surface waves was completed by Ezawa,[2] who constructed an orthogonal complete set of the eigenmodes of elastic waves in a half-space with a stress-free plane boundary. The real surface of the solids, however, is rather rough, so that elastic surface waves will be scattered by the surface irregularities considerably. Therefore, it would be of interest to investigate how the elastic surface waves are scattered by mass defects localized in the solid surface. Scattering of Rayleigh waves by surface-mass defects has already been discussed by Steg and Klemens,[3] who showed, using the perturbative approximation, that the scattering varies as the fifth power of incident frequency.

It is well known that there exists typical resonant scattering of lattice waves by point defects in crystals and that no perturbative approach could reproduce such characteristic behavior of scattering. Many authors[4] have investigated these resonances essentially in terms of the lattice-Green's-function method and it has been clarified that it is important to take into account the higher-order effect of phonon scattering with the point defects. In the presence of the surface boundary, we may also anticipate the resonance scattering of elastic surface waves by point defects localized in the solid surface and we therefore have to take into account the higher-order rescattering effects in calculating the elastic-surface-wave scattering amplitudes. The presence of the surface boundary, however, seems to make it somewhat difficult to obtain the scattering amplitude by means of the lattice-Green's-function method.[5]

In this connection, the present author[6,7] recently proposed an alternative approach to the calculation of the elastic-surface-wave scattering amplitude from the static mass defect, which was originally developed by Chew and Low[8] for meson scattering by a static source. In a previous paper,[7] where we took into account only two modes (the Rayleigh mode and the mode with total reflection) among five modes forming an orthogonal complete set of the eigenmodes, it has been shown that the characteristic resonant structure appears in the scattering cross sections as expected.

In this paper, we generalize this approach to include all of the five modes which form an orthogonal complete set of the eigenmodes of elastic surface waves. Representations for the quantum of elastic surface waves are explicitly given in Sec. II by following Ezawa's work, while in Sec. III the integral equations for the scattering amplitudes are constructed by means of field-theoretical scattering theory. In Sec. IV, we calculate the scattering cross sections by introducing the approximations needed to linearize the integral equations for scattering amplitudes. Results and discussions are given in Sec. V. Throughout this paper, a system of units in which $\hbar = 1$ is used.

II. QUANTIZATION OF ELASTIC SURFACE WAVES

We assume that the crystal can be approximated by an isotropic elastic continuum and that it occupies the half-space $z \geq 0$, with a stress-free plane boundary at $z = 0$. We can expand,[2] as in the bulk-phonon case, the displacement vector $\vec{u}(\vec{r}, t)$ at a point $\vec{r} = (\vec{\rho}, z)$ and a time t in terms of eigenmodes,

$$\vec{u}(\vec{r}, t) = \sum_J 1/(8\pi^2\rho\omega_J)^{1/2}[a_J \vec{u}^{(J)}(z)\, e^{i\vec{\kappa}\cdot\vec{\rho} - i\omega_J t} + a_J^\dagger \vec{u}^{(J)*}(z)\, e^{-i\vec{\kappa}\cdot\vec{\rho} + i\omega_J t}], \quad (2.1)$$

where J represents a set of three quantum numbers, $\vec{\kappa}$ being the wave vector in the x-y plane, c the propagation velocity in the x-y plane ($c = \omega_J/|\vec{\kappa}|$), and m labeling the five eigenmodes of elastic waves in a half-space; that is $J = \{\vec{\kappa}, c, m\}$. ρ is the density of crystal and a_J and $a_J^\dagger$ are the annihilation and creation operators of the J-mode quantum of

elastic surface waves obeying the ordinary commutation relation of the Bose type:

$$[a_J,\ a_{J'}^{\dagger}] = \delta_{J,J'} \ . \tag{2.2}$$

$\vec{\rho}$ is the coordinate vector in the x-y plane.

The five eigenmodes of elastic waves in a half-space, which are denoted by the symbol m, will be shown below[2].

A. Rayleigh Mode ($m=R$)

The Rayleigh mode is a representative surface mode whose amplitude decreases exponentially with the distance from the surface. In this mode, velocity c takes only one value c_R which is given as the solution of the following equation:

$$4[\{1-(c_R/c_t)^2\}\{1-(c_R/c_l)^2\}]^{1/2} = [2-(c_R/c_t)^2]^2 , \tag{2.3}$$

where c_t and c_l are, respectively, the transverse and longitudinal sound velocities in bulk crystals: Eq. (2.3) is known to have a single positive root which is slightly smaller than c_t. The dispersion relation gives $\omega_J = c_R \kappa$. Then we have the following wave functions for the Rayleigh mode;

$$\begin{aligned} u_1^{(R)}(z) &= i\frac{\kappa_1}{\kappa}\left(\frac{\kappa}{K}\right)^{1/2}\left(e^{-\gamma\kappa z} - \frac{2\gamma\eta}{1+\eta^2}e^{-\eta\kappa z}\right), \\ u_2^{(R)}(z) &= i\frac{\kappa_2}{\kappa}\left(\frac{\kappa}{K}\right)^{1/2}\left(e^{-\gamma\kappa z} - \frac{2\gamma\eta}{1+\eta^2}e^{-\eta\kappa z}\right), \\ u_3^{(R)}(z) &= -\left(\frac{\kappa}{K}\right)^{1/2}\left(e^{-\gamma\kappa z} - \frac{2}{1+\eta^2}e^{-\eta\kappa z}\right), \end{aligned} \tag{2.4}$$

where

$$\gamma = [1-(c_R/c_l)^2]^{1/2}, \quad \eta = [1-(c_R/c_t)^2]^{1/2} \ , \tag{2.5}$$

and

$$K = (\gamma-\eta)(\gamma-\eta-2\gamma\eta^2)/2\gamma\eta^2 \ . \tag{2.6}$$

B. Mode with Total Reflection ($m=T$)

This is the mode with longitudinal and transverse waves. The longitudinal part is localized in the surface as in the Rayleigh mode. In this mode, c takes the continuous values between c_t and c_l, and we have for the mode with total reflection,

$$\begin{aligned} u_1^{(T)}(z) &= i\frac{\kappa_1}{\kappa}\left(\frac{\kappa}{2\pi c\beta}\right)^{1/2}[C\,e^{-\alpha\kappa z} + \beta(e^{-i\beta\kappa z} + A\,e^{i\beta\kappa z})] \ , \\ u_2^{(T)}(z) &= i\frac{\kappa_2}{\kappa}\left(\frac{\kappa}{2\pi c\beta}\right)^{1/2}[C\,e^{-\alpha\kappa z} + \beta(e^{-i\beta\kappa z} + A\,e^{i\beta\kappa z})] \ , \\ u_3^{(T)}(z) &= \left(\frac{\kappa}{2\pi c\beta}\right)^{1/2}[-\alpha C\,e^{-\alpha\kappa z} + i(e^{-i\beta\kappa z} - A\,e^{i\beta\kappa z})] \ , \end{aligned} \tag{2.7}$$

where

$$\begin{aligned} &\alpha = [1-(c/c_t)^2]^{1/2}, \quad \beta = [(c/c_t)^2-1]^{1/2}, \\ &A = \frac{(\beta^2-1)^2 - 4i\alpha\beta}{(\beta^2-1)^2 + 4i\alpha\beta} \ , \end{aligned} \tag{2.8}$$

and

$$C = \frac{4\beta(\beta^2-1)}{(\beta^2-1)^2 + 4i\alpha\beta} \ .$$

C. Mixed Pressure-Shear-Wave Modes ($m=\pm$)

These modes consist of pressure wave (P mode) and shear wave with vertical polarization (SV mode), which interact with each other through the surface. A proper combination of these modes will give two orthogonal eigenmodes; that is, $m=\pm$. In these modes, c takes the continuous values greater than c_l, and we have for the mixed P-SV modes,

$$\begin{aligned} u_1^{(\pm)}(z) &= \frac{\kappa_1}{\kappa}\left(\frac{\kappa}{4\pi c}\right)^{1/2}\left(\mp\frac{1}{\delta^{1/2}}(e^{-i\delta\kappa z} - \zeta_{\pm}e^{i\delta\kappa z}) \right. \\ &\qquad \left. + i\beta^{1/2}(e^{-i\beta\kappa z} + \zeta_{\pm}e^{i\beta\kappa z})\right), \\ u_2^{(\pm)}(z) &= \frac{\kappa_2}{\kappa}\left(\frac{\kappa}{4\pi c}\right)^{1/2}\left(\mp\frac{1}{\delta^{1/2}}(e^{-i\delta\kappa z} - \zeta_{\pm}e^{i\delta\kappa z}) \right. \\ &\qquad \left. + i\beta^{1/2}(e^{-i\beta\kappa z} + \zeta_{\pm}e^{i\beta\kappa z})\right), \\ u_3^{(\pm)}(z) &= \left(\frac{\kappa}{4\pi c}\right)^{1/2}\left(\pm\delta^{1/2}(e^{-i\delta\kappa z} + \zeta_{\pm}e^{i\delta\kappa z}) \right. \\ &\qquad \left. + \frac{i}{\beta^{1/2}}(e^{-i\beta\kappa z} - \zeta_{\pm}e^{i\beta\kappa z})\right), \end{aligned} \tag{2.9}$$

where

$$\begin{aligned} &\delta = [(c/c_l)^2-1]^{1/2}, \quad \zeta_{\pm} = D \pm iB \ , \\ &D = \frac{(\beta^2-1)^2 - 4\delta\beta}{(\beta^2-1)^2 + 4\delta\beta} \ , \end{aligned} \tag{2.10}$$

and

$$B = \frac{4\sqrt{\delta\beta}(\beta^2-1)}{(\beta^2-1)^2 + 4\delta\beta} \ .$$

D. Shear Wave with Horizontal Polarization Mode ($m=SH$)

This mode is the shear wave with horizontal polarization; that is, $m=SH$. In this mode, c takes the continuous values greater than c_t, and we have for the SH mode,

$$\begin{aligned} u_1^{(SH)}(z) &= -\frac{\kappa_2}{\kappa}\left(\frac{2c\kappa}{\pi c_t^2\beta}\right)^{1/2}\cos\beta\kappa z \ , \\ u_2^{(SH)}(z) &= \frac{\kappa_1}{\kappa}\left(\frac{2c\kappa}{\pi c_t^2\beta}\right)^{1/2}\cos\beta\kappa z \ , \\ u_3^{(SH)}(z) &= 0 \ . \end{aligned} \tag{2.11}$$

It has been shown by Ezawa that the above-mentioned five modes construct an orthonormal and complete set of eigenmodes and that the definition of the summation over J in (2.1) should be

$$\sum_J f(\vec{\kappa},\ c,\ m) = \int d\vec{\kappa} \left(\sum_{m \neq R} \int_{\Gamma_m} dc\, f(\vec{\kappa},\ c,\ m) + f(\vec{\kappa},\ c_R,\ R) \right), \quad (2.12)$$

where Γ_m indicates the region in which the integration over c must be done. The symbolic expression $\delta_{J,J'}$ in (2.2) should also be understood to be

$$\delta_{J,J'} = \delta_{m,m'} \delta(\vec{\kappa} - \vec{\kappa}') \delta(c - c') \quad (2.13)$$

when c and c' belong to the continuous spectrum, and

$$\delta_{J,J'} = \delta_{m,m'} \delta(\vec{\kappa} - \vec{\kappa}') \delta_{c,c'} \quad (2.14)$$

when either c or c' belong to the discrete spectrum.

III. FORMULATION

If we assume the crystals to be an isotropic elastic continuum, the elastic energy of the crystal is given by

$$H = \frac{1}{2} \int \rho(\vec{r}) \left(\frac{\partial \vec{u}}{\partial t} \right)^2 d\vec{r} + V_h \ , \quad (3.1)$$

where $\rho(\vec{r})$ is the mass density and V_h the harmonic potential. We consider the point-mass defect localized in the solid surface and then the mass density $\rho(\vec{r})$ can be written in the following form:

$$\rho(\vec{r}) = \bar{\rho} + \rho(\vec{r}) - \bar{\rho} = \bar{\rho} + \Delta M \delta(\vec{r}) \ , \quad (3.2)$$

where $\bar{\rho}$ is the average mass density of crystal. Then the Hamiltonian (3.1) is split into two parts—free Hamiltonian H_0 and interaction Hamiltonian H'—of the elastic surface wave, with the point-mass defect localized at the origin,

$$H = H_0 + H' \ , \quad (3.3)$$

where

$$H_0 = \frac{\bar{\rho}}{2} \int \left(\frac{\partial \vec{u}}{\partial t} \right)^2 d\vec{r} + V_h \quad (3.4)$$

and

$$H' = \frac{\Delta M}{2} \left(\frac{\partial \vec{u}}{\partial t} \right)^2 \Big|_{\vec{r}=0} \ . \quad (3.5)$$

It will be easily seen that the free Hamiltonian H_0 can be diagonalized by inserting the eigenmode expansion (2.1) into (3.4):

$$H_0 = \sum_J \hbar \omega_J (a_J^\dagger a_J + \tfrac{1}{2}) \ . \quad (3.6)$$

Similarly, we obtain the interaction Hamiltonian of the elastic surface wave with point-mass defect statically localized in the solid surface in terms of annihilation and creation operators:

$$H' = -\frac{\Delta M}{8\pi\rho} \sum_{J,J'} (\omega_J \omega_{J'})^{1/2} [a_J\, a_{J'} (\vec{u}^{(J)}(0) \cdot \vec{u}^{(J')}(0)) - a_J\, a_{J'}^\dagger (\vec{u}^{(J)}(0) \cdot \vec{u}^{(J')*}(0)) + \text{H.c.}]. \quad (3.7)$$

The total Hamiltonian has a complete set of eigenstates $\{|\psi_n\rangle\}$. Among these states, we are particularly interested in the one J-mode quantum state produced by elastic surface waves + single-mass defects with outgoing or incoming waves $|\psi_J^{(\pm)}\rangle$. Thus, in complete analogy to the work by Chew and Low,[8] we can readily obtain the formal solution for $|\psi_J^{(\pm)}\rangle$ in the following form:

$$|\psi_J^{(\pm)}\rangle = a_J^\dagger |\psi_0\rangle - [1/(H - \omega_J \mp i\epsilon)]\, V_J |\psi_0\rangle \ , \quad (3.8)$$

where

$$V_J = [\, H', a_J^\dagger \,] \ . \quad (3.9)$$

Writing Eq. (3.8), the single-mass-defect state $|\psi_0\rangle$ has been chosen to have zero energy:

$$H|\psi_0\rangle = 0 \ ,$$
$$H|\psi_J^{(\pm)}\rangle = \omega_J |\psi_J^{(\pm)}\rangle \ , \quad \text{etc.} \quad (3.10)$$

Furthermore, it would be worthy to note that we can obtain the following equation similarly:

$$a_J |\psi_0\rangle = -[1/(H + \omega_J)]\, V_J^\dagger |\psi_0\rangle \ . \quad (3.11)$$

We start with the following scattering matrix in which the J-mode quantum is scattered into the J'-mode quantum by point-mass defect:

$$S_{J',J} = \langle \psi_{J'}^{(-)} | \psi_J^{(+)} \rangle \ . \quad (3.12)$$

Inserting (3.8) into (3.12) and proceeding in the manner of Chew and Low, we find

$$S_{J',J} = \delta_{J',J} - 2\pi i \delta(\omega_{J'} - \omega_J) T_{J',J} \ , \quad (3.13)$$

where

$$T_{J',J} = \langle \psi_{J'}^{(-)} | V_J | \psi_0 \rangle \ . \quad (3.14)$$

In the energy shell this is the conventional scattering amplitude. Here one might notice that $V_J^\dagger$ is equal to neither V_J nor $-V_J$ and, consequently, another independent transition amplitude $R_{J',J}$ must be defined:

$$R_{J',J} = \langle \psi_{J'}^{(-)} | V_J^\dagger | \psi_0 \rangle \ . \quad (3.15)$$

Diagrams for the amplitudes $T_{J',J}$ and $R_{J',J}$ are shown in Fig. 1.

We now insert (3.8) into (3.14) and (3.15) and, using the completeness condition, introduce the complete set of eigenstates $|\psi_n^{(-)}\rangle$. The index n indicates the quantum state of elastic surface waves as well as the number present. Then the equations for the two independent amplitudes $T_{J',J}$ and $R_{J',J}$ are given by

$$T_{J',J} = T_{J',J}^B - \sum_n \left(\frac{R_{nJ}^* R_{nJ'}}{\omega_n + \omega_{J'}} + \frac{T_{nJ'}^* T_{nJ}}{\omega_n - \omega_{J'} - i\epsilon} \right) \quad (3.16)$$

and

$$R_{J',J} = R_{J',J}^B - \sum_n \left(\frac{T_{nJ}^* R_{nJ'}}{\omega_n + \omega_{J'}} + \frac{T_{nJ'}^* R_{nJ}}{\omega_n - \omega_{J'} - i\epsilon} \right) , \quad (3.17)$$

where

$$T^B_{J'J} = \langle \psi_0 | [a_{J'}, V_J] | \psi_0 \rangle \tag{3.18}$$

and

$$R^B_{J'J} = \langle \psi_0 | [a_{J'}, V^\dagger_J] | \psi_0 \rangle .$$

If we assume that the emission probabilities of more than one quantum of elastic surface waves from static-mass defects are small compared with that of one quantum, then the contributions of multiquantum states to the integral equations (3.16) and (3.17) may be neglected. It is possible, in principle, to estimate the contributions of more than one quantum-intermediate state by solving the similar integral equations for amplitude-amplifying the elastic surface waves simultaneously. This will, however, be reserved as a future problem:

$$T_{J'J} = T^B_{J'J} - \sum_{J''} \left(\frac{R^*_{J''J} R_{J''J'}}{\omega_{J''} + \omega_{J'}} + \frac{T^*_{J''J'} T_{J''J}}{\omega_{J''} - \omega_{J'} - i\epsilon} \right) , \tag{3.19a}$$

$$R_{J'J} = R^B_{J'J} - \sum_{J''} \left(\frac{T^*_{J''J} R_{J''J'}}{\omega_{J''} + \omega_{J'}} + \frac{T^*_{J''J'} R_{J''J}}{\omega_{J''} - \omega_{J'} - i\epsilon} \right) . \tag{3.19b}$$

Equations (3.19a) and (3.19b) are the so-called multichannel self-consistent bootstrap equations used to determine the scattering amplitudes and are illustrated graphically in Fig. 2.

IV. SCATTERING AMPLITUDES AND CROSS SECTIONS

Since Eqs. (3.19a) and (3.19b) are the simultaneous nonlinear integral equations for $T_{J'J}$ and

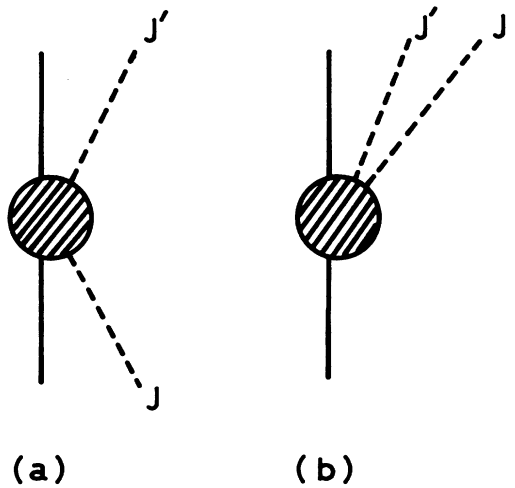

FIG. 1. Diagrams (a) and (b) illustrating $T_{J'J}$ and $R_{J'J}$, respectively. The solid line refers to mass defect and the dashed line to surfon. The shaded circle represents the complete physical interaction.

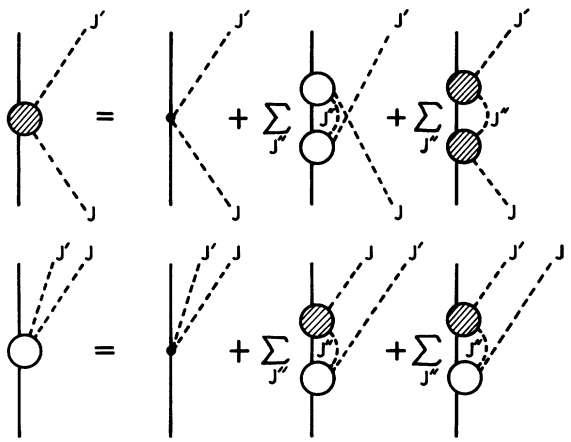

FIG. 2. Graphical schemes for the simultaneous integral equations (3.19a) and (3.19b). The open and shaded circles refer to the transition amplitudes $R_{J'J}$ and $T_{J'J}$, respectively. The solid circle stands for the amplitude in the Born approximation.

$R_{J'J}$, it is difficult to find an exact solution. Therefore we introduce some approximations which maintain the essential features of the amplitudes in order to simplify the equations and see whether or not the solution has the resonance structure. First, we may safely neglect the first term in the large parentheses of the right-hand side, because the energy denominator of that term does not have zero. Consequently, we need not solve the integral equation for $R_{J'J}$ and need only consider the following integral equation relevant to the scattering amplitude $T_{J'J}$:

$$T_{J'J} = T^B_{J'J} - \sum_{J''} \frac{T^*_{J''J'} T_{J''J}}{\omega_{J''} - \omega_{J'} - i\epsilon} . \tag{4.1}$$

Second, as mentioned in Sec. I, it is essential to take into account the higher-order rescattering effect in calculating the scattering amplitude. We therefore introduce the second approximation, which replaces one of the scattering amplitudes in the integral with the amplitude in the Born approximation:

$$T_{J'J} = T^B_{J'J} - \sum_{J''} \frac{T^{B*}_{J''J'} T_{J''J}}{\omega_{J''} - \omega_{J'} - i\epsilon} . \tag{4.2}$$

This approximation allows the amplitude to include all orders of rescattering effects, as illustrated in Fig. 3. Furthermore, it has already been ascertained that this approximation gives a qualitatively correct scattering amplitude in the case of meson scattering by a static source.

Then, the solution of multichannel integral equations (4.2) can easily be obtained by the standard method and we have the following expressions for the scattering amplitudes of the Rayleigh-mode incident wave:

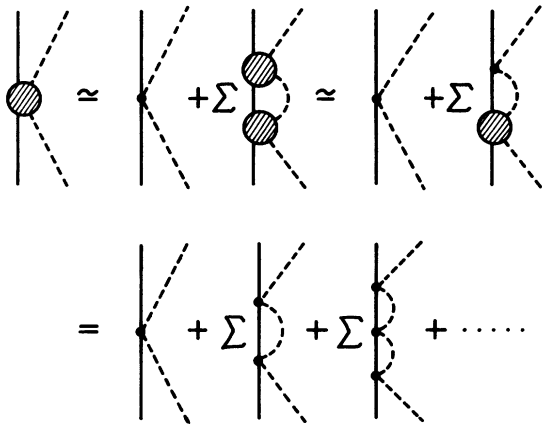

FIG. 3. Graphical schemes for the approximated equation (4.2). The shaded circle refers to the physical scattering amplitude $T_{J'J}$. The solid circle stands for the amplitude in the Born approximation.

$$T_{J'J}=\frac{\Delta M}{8\pi\rho}\,(\omega_J\omega_{J'})^{1/2}\left(\sum_{i=1}^{2}u_i^{(J)}(0)u_i^{(J')*}(0)\frac{N^{(J'J)}}{D}+u_3^{(J)}(0)u_3^{(J)*}(0)\frac{N'^{(J'J)}}{D'}\right), \tag{4.3}$$

where D, D', $N^{(J'J)}$, and $N'^{(J'J)}$ will be given below:

$$D=(1-a)(1-b)(1-c)(1+d)+4c(1-a)(1-b)(1-d)+2a(1-b)(1-c)(1-d)+2b(1-a)(1-c)(1-d), \tag{4.4}$$

$$D'=(1-a')(1-b')(1-c')+4c'(1-a')(1-b')+2a'(1-b')(1-c')+2b'(1-a')(1-c').$$

For the scattering process

$$R+\Delta M\rightarrow R+\Delta M, \tag{4.5}$$

we have

$$N^{(J'J)}=1-3(b+d)-5(c-bd)+7c(b+d)-9bcd, \tag{4.6}$$

$$N'^{(J'J)}=1-3b'-5c'+7b'c'.$$

For the process

$$R+\Delta M\rightarrow T+\Delta M, \tag{4.7}$$

we have

$$N^{(J'J)}=2(1-c)(1-d),\qquad N'^{(J'J)}=2(1-c'). \tag{4.8}$$

For the process

$$R+\Delta M\rightarrow(\pm)+\Delta M, \tag{4.9}$$

we have

$$N^{(J'J)}=2(1-b)(1-d),\qquad N'^{(J'J)}=2(1-b'). \tag{4.10}$$

For the process

$$R+\Delta M\rightarrow SH+\Delta M, \tag{4.11}$$

we have

$$N^{(J'J)}=2(1-b)(1-c),\qquad N'^{(J'J)}=0. \tag{4.12}$$

a, b, c, and d are functions of incident frequency and are given in the following:

$$a=FD_1f(x),\quad a'=FD_2f(x),\quad b=FC_1f(x),\quad b'=FC_2f(x),\quad c=FG_1f(x),\quad c'=FG_2f(x),\quad d=FLf(x), \tag{4.13}$$

where

$$F=\frac{\Delta M}{2\pi\rho}\left(\frac{\omega_m}{c_R}\right)^3,$$

$$f(x)=\tfrac{1}{2}+\tfrac{1}{3}x+x^2+x^3\ln\left(\frac{1-x}{x}\right)+i\pi x^3,$$

and

$$x=\omega/\omega_m.$$

ω is the incident wave frequency of the Rayleigh mode and ω_m the maximum frequency corresponding to the Debye frequency in the bulk-phonon case. C_1, C_2, D_1, D_2, G_1, G_2, and L are some dimensionless constants which depend upon c_l, c_t, and c_R:

$$C_1=\frac{c_R^3}{2}\int_{c_t}^{c_l}dc\;\frac{\beta(\beta^4-1)^2}{c^4[(\beta^2-1)^4+16\alpha^2\beta^2]},$$

$$C_2=4c_R^3\int_{c_t}^{c_l}dc\;\frac{\alpha^2\beta(\beta^2+1)^2}{c^4[(\beta^2-1)^4+16\alpha^2\beta^2]},$$

$$D_1=\frac{\pi}{4K}\left(1-\frac{2\gamma\eta}{1+\eta^2}\right)^2,$$

$$D_2=\frac{\pi}{2K}\,\gamma^2\left(1-\frac{2}{1+\eta^2}\right)^2, \tag{4.14}$$

$$G_1=\frac{c_R^3}{8}\int_{c_l}^{\infty}\frac{dc}{c^4}\left[\frac{1}{\delta}(1-A)+\beta(1+A)+2\left(\frac{\beta}{\delta}\right)^{1/2}B\right],$$

$$G_2=\frac{c_R^3}{4}\int_{c_l}^{\infty}\frac{dc}{c^4}\left[\delta(1+A)+\frac{1}{\beta}(1-A)+2\left(\frac{\delta}{\beta}\right)^{1/2}B\right],$$

$$L=\frac{c_R^3}{2c_t^2}\int_{c_t}^{\infty}\frac{dc}{c^2\beta}.$$

The scattering cross section for the J-mode to that of the J'-mode wave is given by

$$\sigma_{J\rightarrow J'}=\frac{2\pi}{v}\sum_{J'}{}'\,\delta(\omega_{J'}-\omega_J)\,|T_{J'J}|^2, \tag{4.15}$$

where the prime over $\sum$ means that summation over mode index m' is not to be taken. Inserting the explicit expression for amplitude (4.3) into (4.15), we obtain the following expressions for various cross sections:

$$\sigma_{R\to R} = 2D_1^2 F^2 x^5 \left(\frac{c_R}{\omega_m}\right) \times\left(\frac{|N^{(RR)}|^2}{|D|^2} + \frac{\frac{1}{2}(D_2/D_1)^2 |N'^{(RR)}|^2}{|D'|^2}\right) , \quad (4.16)$$

$$\sigma_{R\to T} = 2C_1 D_1 F^2 x^5 \left(\frac{c_R}{\omega_m}\right) \times\left(\frac{|N^{(TR)}|^2}{|D|^2} + \frac{\frac{1}{2}(C_2 D_2/C_1 D_1) |N'^{(TR)}|^2}{|D'|^2}\right) , \quad (4.17)$$

$$\sigma_{R\to P} = D_1 H_1 F^2 x^5 \left(\frac{c_R}{\omega_m}\right) \times\left(\frac{|N^{(\pm R)}|^2}{|D|^2} + \frac{(D_2 H_1'/D_1 H_1) |N'^{(\pm R)}|^2}{|D'|^2}\right) , \quad (4.18)$$

$$\sigma_{R\to SV} = D_1 H_2 F^2 x^5 \left(\frac{c_R}{\omega_m}\right) \times\left(\frac{|N^{(\pm R)}|^2}{|D|^2} + \frac{(D_2 H_1/D_1 H_2) |N'^{(\pm R)}|^2}{|D'|^2}\right) , \quad (4.19)$$

$$\sigma_{R\to SH} = 2D_1 L F^2 x^5 \left(\frac{c_R}{\omega_m}\right) \frac{|N^{(HR)}|^2}{|D|^2} . \quad (4.20)$$

where H_1, H_2, and H_1' are also dimensionless constants depending on c_t, c_l, and c_R:

$$H_1 = \frac{c_R^3}{8} \int_{c_l}^{\infty} dc \, \frac{\delta}{c^4} \left(\frac{1}{\delta^{1/2}} (1-A) + \beta^{1/2} B\right)^2 ,$$

$$H_2 = \frac{c_R^3}{8} \int_{c_l}^{\infty} dc \, \frac{\beta}{c^4} \left(\frac{1}{\delta^{1/2}} B + \beta^{1/2} (1+A)\right)^2 , \quad (4.21)$$

$$H_1' = \frac{c_R^3}{8} \int_{c_l}^{\infty} dc \, \frac{\delta}{c^4} \left(\delta^{1/2} (1+A) + \frac{1}{\beta^{1/2}} B\right)^2 .$$

Frequency-dependent parts in the large parentheses on the right-hand side of Eqs. (4.16)–(4.20) represent the higher-order rescattering effect of elastic surface waves with static-mass defect and thus it is seen that scattering in lowest-order perturbation theory is proportional to $(\Delta M)^2 \omega^5$, as predicted by Steg and Klemens.[3]

V. RESULTS AND DISCUSSIONS

Now, in order to see an actual frequency dependence of the cross sections (4.16)–(4.20), we take, for example, the following values of parameters for silicon:

$$\rho = 2.5 \text{ g cm}^{-3}, \quad c_R = 4.9\times10^5 \text{ cm sec}^{-1} , \quad (5.1)$$
$$c_t = 5.3\times10^5 \text{ cm sec}^{-1}, \quad c_l = 9.5\times10^5 \text{ cm sec}^{-1} .$$

In this case, the dimensionless constants defined in (4.14) and (4.21) give the following numerical values:

$$C_1 = 0.0361 , \quad C_2 = 0.1981 ,$$
$$D_1 = 0.1048 , \quad D_2 = 0.4639 ,$$
$$G_1 = 0.0796 , \quad G_2 = 0.0618 ,$$
$$L = 0.3235 , \quad H_1 = 0.0401 ,$$
$$H_2 = 0.3751 , \quad H_1' = 0.0865 .$$

As for the value of maximum frequency ω_m, we assume two different values:

$$\omega_m = 0.75\times10^{14} \text{ sec}^{-1} , \quad (5.2a)$$
$$\omega_m = 1.0\times10^{14} \text{ sec}^{-1} . \quad (5.2b)$$

Using the above numerical values, we show in Figs. 4(a) and 4(b) the scattering cross sections as functions of incident wave frequency together with the cross sections in the Born approximation.

In Fig. 4(a), in which ω_m is assumed to be 0.75×10^{14} sec^{-1}, the cross sections are illustrated for the value of mass difference $\Delta M = -12m$, where m is the neutron mass. We have typical resonance scattering for all the cross sections at resonance frequency $\omega_r \simeq 0.2\times10^{14}$ sec^{-1}, except for the cross section $\sigma_{R\to SH}$. The numerical value of $\sigma_{R\to SH}$ is too small to write in the figure. In case (5.2a) there appears typical resonance structure in the cross sections except in $\sigma_{R\to SH}$ for the range of mass difference $9m \leq -\Delta M \leq 17m$ and resonance frequency ω_r is in the region 0.06×10^{14} sec$^{-1} \lesssim \omega_r \lesssim 0.3\times10^{14}$ sec^{-1}. In Fig. 4(b), where ω_m is assumed to be 10^{14} sec^{-1}, the cross sections behave in quite a similar way. The cross sections for the value of mass difference $\Delta M = -6m$ are illustrated and we find similar resonance structure in the cross sections at $\omega_r \simeq 0.16\times10^{14}$ sec^{-1}, except in the cross section $\sigma_{R\to SH}$. For this value of maximum frequency, we have a resonance structure for the range of mass difference $4m \leq -\Delta M \leq 7m$ and ω_r is in the region 0.09×10^{14} sec$^{-1} \lesssim \omega_r \lesssim 0.35\times10^{14}$ sec^{-1}.

In both cases (5.2a) and (5.2b), it should be noted that the cross section $\sigma_{R\to R}$ is predominantly enhanced and this result is quite plausible because the mass defect has been assumed to be localized in the solid surface. To clarify this situation of enhancement, it would be convenient to define the partition ratio as follows:

$$R_1 = \sigma_{R\to T}/\sigma_{R\to R} , \quad R_2 = \sigma_{R\to P}/\sigma_{R\to R} ,$$
$$R_3 = \sigma_{R\to SV}/\sigma_{R\to R} , \quad R_4 = \sigma_{R\to SH}/\sigma_{R\to R} .$$

The partition ratios R_1 through R_4 are illustrated in Figs. 5(a) and 5(b) together with ratios in the Born approximation as functions of incident frequency.

It is readily seen in Eqs. (4.16)–(4.20) that the partition ratios in the Born approximation are fre-

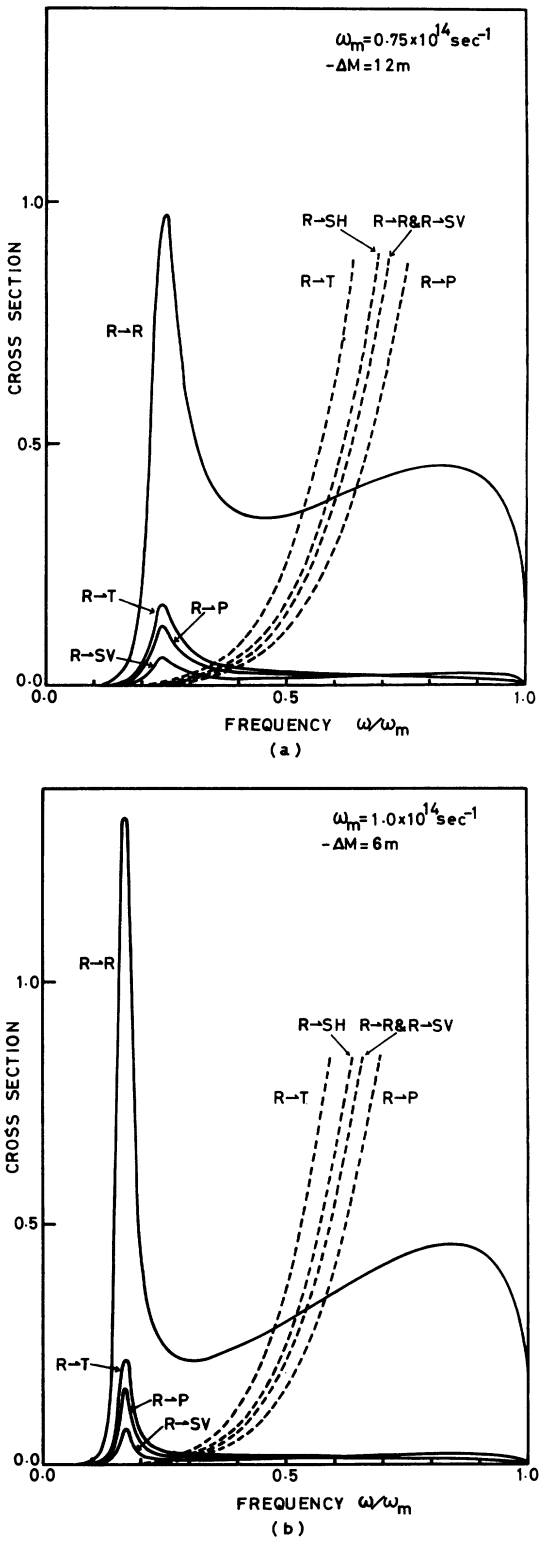

FIG. 4. Scattering cross sections as a function of frequency in the unit ω_m. (a) $\omega_m = 0.75 \times 10^{14}$ sec^{-1} ($\Delta M = -12m$); (b) $\omega_m = 1.0 \times 10^{14}$ sec^{-1} ($\Delta M = -6m$). m is the neutron mass. The dashed lines refer to cross sections in the Born approximation.

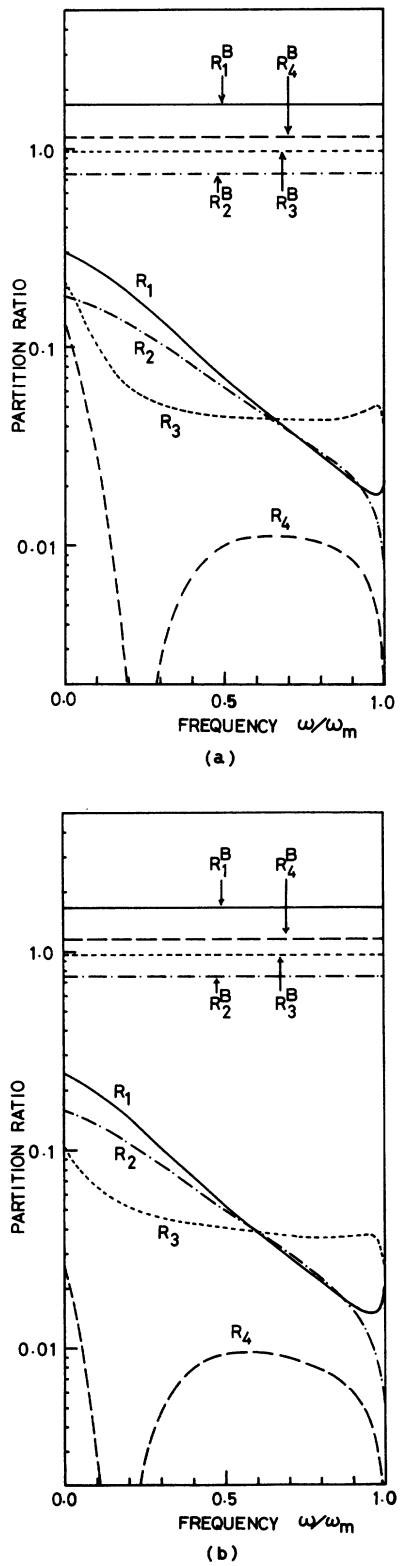

FIG. 5. Partition ratio as a function of frequency in the unit ω_m. (a) $\omega_m = 0.75 \times 10^{14}$ sec^{-1} ($\Delta M = -12m$); (b) $\omega_m = 1.0 \times 10^{14}$ sec^{-1} ($\Delta M = -6m$).

quency independent and take following values:

$$R_1^B = 1.68\ , \quad R_2^B = 0.75\ ,$$

$$R_3^B = 0.98\ , \quad R_4^B = 1.14\ ,$$

where superscript B refers to the Born approximation. If, on the other hand, we take into account the higher-order rescattering effects, the partition ratios decrease considerably and give the values rather smaller than unity, as is seen in Figs. 5(a) and 5(b). These characteristic results are completely consistent with the results obtained in Ref. 7, in which only two modes, R and T, were involved. Moreover, it is noteworthy that there appears no resonance in the scattering process $R + \Delta M \rightarrow SH + \Delta M$.

In conclusion, we have investigated the scattering of elastic surface waves from static point-mass defect localized in the solid surface by solving approximately the so-called Chew-Low equation. We would like to emphasize the following two points. First, resonance structure appears in all the cross sections but $\sigma_{R \rightarrow SH}$ for a static surface defect of lighter mass than that of the host atoms. Second, the inclusion of the rescattering effects of elastic surface waves with mass defect appreciably enhances the scattering into other Rayleigh-mode waves.

The numerical calculations were performed using a FACOM 230-60 computer at the Computer Center of Hokkaido University.

[1]H. Ezawa, T. Kuroda, and K. Nakamura, Surf. Sci., 24, 654 (1971); H. Ezawa, S. Kawaji, T. Kuroda, and K. Nakamura, Surf. Sci. 24, 649 (1971); H. Ezawa, S. Kawaji, and K. Nakamura, Surf. Sci. 27, 218 (1971); S. Kawaji, H. Ezawa, and K. Nakamura, International Conference on Solid Surface, Boston, 1971 (unpublished); J. Vac. Sci. Technol. 9, 762 (1972).

[2]H. Ezawa, Ann. Phys. 67, 438 (1971). In this article, Ezawa named the quantum of elastic surface waves "surfon."

[3]R. G. Steg and P. G. Klemens, Phys. Rev. Lett. 24, 381 (1970).

[4]S. Takeno, Prog. Theor. Phys. 29, 191 (1963); M. V. Klein, Phys. Rev. 131, 1500 (1963); J. Callaway, Nuovo Cimento 29, 883 (1963); R. J. Elliot and D. W. Taylor, Proc. Phys. Soc. 83, 189 (1964); J. A. Krumhansl, in *Proceedings of the International Conference on Lattice Dynamics, Copenhagen*, 1963, edited by R. F. Wallis (Pergamon, Oxford, England, 1965), p. 523; M. Yussouff and J. Mahanty, Proc. Phys. Soc. 85, 1223 (1965); B. K. Agarwal, J. Phys. 2, 252 (1969).

[5]M. Ashkin, Phys. Rev. 136, B821 (1964).

[6]T. Nakayama and T. Sakuma, Lett. Nuovo Cimento 2, 1104 (1971).

[7]T. Sakuma, Phys. Rev. Lett. 29, 1394 (1972).

[8]G. F. Chew and F. E. Low, Phys. Rev. 101, 1570 (1956).

PHYSICAL REVIEW B VOLUME 8, NUMBER 4 15 AUGUST 1973

Molecular-Orbital Studies of As_2S_3 and As_2Se_3

Inan Chen

Xerox Rochester Research Center, Rochester, New York 14644

(Received 12 February 1973)

The basis hybrid orbitals of As_2S_3 and As_2Se_3 for the molecular-orbital calculation of the layer molecules have been investigated. One feature distinct from and one similar to amorphous Se is observed. The former is the inequivalence of the nearest-neighbor σ bonds, which can be interpreted as a reason for low carrier mobilities in these solids. The similar feature is the locations of the bonding and the lone-pair states. As in Se, these are intermixed; thus band-gap photons can break σ bonds, which accounts for the photodissociation and photocrystallization of chalcogenide glasses.

I. INTRODUCTION

In a recent paper[1] the electronic states of a molecular solid—amorphous selenium—has been successfully interpreted by molecular-orbital (MO) theory. In that paper, the calculation of the electronic states of the solid is carried out in three steps. The first step is the identification of the building block, or the basis orbitals for the molecular states. The second step is the calculation of the molecular orbitals by a semiempirical (extended Hueckel) method,[2] including as many units as the convergence requires. Finally, the electronic density of states in the solid is calculated by assuming a Gaussian distribution of states centered at the molecular states. It is found that the first step has a determinate effect on the density of states in the solids, e.g., only when the bonding and antibonding orbitals between two neighboring atoms, and the lone-pair hybrid orbitals are chosen as bases for the MO calculations, the calculated density of states agrees with that obtained from